Responses to Referee #2

Thank you for reading the manuscript and providing very useful comments and suggestions to improve the paper. The referee comments are in black, while our replies are in blue. The modifications in the revised manuscript can be found in the track change version of manuscript.

This manuscript describes an innovative data fusion study that derives intrinsic and extrinsic properties of wildfire smoke using a combination of Aeolus/ALADIN measurements combined with ancillary measurements obtained from CALIPSO/CALIOP, MODIS and VIIRS, and informed by MERRA2 model data. Although ALADIN is a space-based HSRL that can directly estimate altitude-resolved extinction coefficients, it only measures the parallel component of the lidar backscatter. The perpendicular component required to estimate the total backscatter coefficient is derived from CALIOP particulate depolarization ratio retrievals for "smoke-related" aerosol types. To differentiate between aerosol and cloud and between smoke and other aerosol types, the authors use passive sensor measurements from MODIS and VIIRS, together with smoke column mass concentrations reported by MERRA2. They then use the revised smoke optical properties measured over a one-week time period (14–21 September 2022) to map smoke transport and characterize changes in smoke optical properties. I enjoyed reading this paper, and after the authors make some (fairly substantial?) modifications, it should be suitable for publication. However, given that an entirely new retrieval scheme is introduced, the subject matter may be more appropriately published in AMT rather than in ACP.

AR: Many thanks for your detailed review and your keen insights into both the methodology and the results of our study. We greatly benefited from working through your comments and found much inspiration while revising the manuscript. In light of your suggestions, we have made substantial revisions. We carefully considered all your advice and have incorporated almost all of it into the revised version.

Inspired by your and Referee #3's concerns, major modifications on the structure has been made: 1) the title has been revised as "Characterization of aerosol properties during a huge transatlantic smoke transport event using Aeolus observations in synergy with multi-platform data";

2) A new Section 4.3 "Caveats and uncertainties" has been added to be dedicated for the discussion for the caveats and potential uncertainties associated with deriving the smoke dataset;

3) more sub-sections were set in Section 5 for result analysis and discussion:

- 5.1 Cross-sections of the smoke aerosol layers at different transport stages
    - 5.1.1 General transport pathway analysis by the cross-sections
    - 5.1.2 Characteristics of the smoke layers at different transport stages
- 5.2 Characteristics of the smoke aerosol plume across its entire transport
    - 5.2.1 Variation of smoke aerosol optical depth and altitude along the longitude
    - 5.2.2 Investigation of the two branches following plume separation
    - 5.2.3 Variation of lidar ratio along the longitude

The revised manuscript continues to focus on the smoke transport event, with the methodology and results structured around this central theme. The characterization of aerosols has been substantially enriched in response to your feedback. We believe the manuscript is now suitable for publication in ACP.

Please find below our point-by-point responses to your comments. We sincerely look forward to your further evaluation and favorable consideration.

My major comments are as follows:

1. I am uneasy about the authors' method for obtaining total backscatter coefficients and their associated uncertainties. Surely the method they've chosen is straightforward: $\beta_{total}(z) = (1+\delta) \times \beta_{//}(z)$, where $\beta_{//}(z)$ is the parallel channel particulate backscatter coefficient reported in the ALADIN Level 2A (L2A) data products and δ is a mean particulate depolarization ratio computed from aggregated CALIOP particulate depolarization ratio estimates. The authors use the L2A extinction and *parallel channel* backscatter coefficients generated by the MLE algorithm described by Ehlers et al., 2022. And, according to that paper, "particle backscatter and extinction coefficients are retrieved in a coupled way" (emphasis added). Consequently, I would think that the best estimates of *total* backscatter coefficients would be obtained by adapting the MLE to ingest depolarization ratio estimates. Doing this would require accounting for the assumed particulate depolarization ratio in the input vector and, importantly, in the covariance matrix. Furthermore, since this would be a nonlinear regression problem, I do not assume that the propagation of depolarization uncertainties into the retrieved backscatter and extinction coefficients would necessarily follow the simple linear model proposed by the authors. While my disquiet may well be misplaced, given that backscatter and extinction are indeed "coupled" quantities, I believe it is incumbent on the authors to offer convincing evidence to dissuade me.

AR: Thanks for your keen insight and the original idea for the total backscatter coefficients retrieval. It would be a significant and general method for the Aeolus L2A products retrieval to consider depolarization ratio as one of the inputs to the MLE algorithm. However, the main purpose of this manuscript is **not to develop the basic algorithm**, but to **characterize one smoke transport event by exploiting the public Aeolus L2A products** in synergy with multi-platform data. The **methodology** developed and used in this manuscript was **derived from, or is related to, the characteristic features** of this smoke transport event, specifically its low and stable depolarization ratio.

We admit the method for obtaining total backscatter coefficients used in this manuscript is quite straightforward. The initial motivation of using Aeolus products for observation of a smoke transport in troposphere was that **the smoke aerosol particles should be more spherical with low and stable depolarization ratio**, so it would be easier to obtain the total backscatter coefficients and the lidar ratios. Although the **smoke depolarization ratios** of this transport event were found larger (0.15 at 355 nm), they were also found **fairly stable during the entire transport** (indicated by the Table A1, also shown below). We only focused on the **mean values of the depolarization ratios**. The largest variation (0.009, from 0.119 to 0.110) of the depolarization ratios could induce the variation of lidar ratio for 0.9 sr, for a typical case illustrated in "4.3 Caveats and uncertainties". It is considered **not significant for the entire variation tendency of lidar ratio during the transport**, which we regarded as an important scientific topic of this manuscript. The variation tendency investigation of the smoke lidar ratio during this transport event would be the first discussion about this issue for the entire smoke transport event. We emphasize that "the corrected results are only used for the mean value analyses of a single measurement cross-section or a specific sub-region in the following discussion" (from "4.3 Caveats and uncertainties"), but not using for each data bins. We also agree this method is too sketchy to apply for each data bins, for which the new MLE method you mentioned might be a better choice.

Longitude ranges of Sub-regions	140°W - 120°W	120°W - 100°W	100°W -80°W	80°W-60°W	60°W-40°W	40°W-20°W	20°W-0°	0°-20°W	20-40°W
Depolarization ratio (mean±std)	0.119± 0.087	0.117± 0.088	0.119± 0.088	0.114± 0.088	0.116± 0.087	0.111± 0.083	0.110± 0.083	0.110± 0.085	0.116± 0.086

Table A1. Depolarization ratio at 532 nm of the smoke plume during transport from 140°to 40°E, derived from CALIOP observations.

The detailed discussion of the backscatter coefficient and lidar ratio uncertainties introduced by the constant linear depolarization ratio is presented below, and was also added into a new dedicated section "4.3 Caveats and uncertainties".

On a related note, I am assuming that the standard deviations reported in Table 1 are the standard deviations that would be calculated by averaging mean values irrespective of their associated uncertainties. One of the wonderful things about HSRLs is that they can retrieve height-resolved estimates of lidar ratios, whereas elastic backscatter systems like CALIOP can, at best, retrieve layer mean values. However, ALADIN's height-resolved lidar ratio estimates have associated height-resolved uncertainties, and these uncertainties will almost certainly grow larger with the introduction of depolarization ratios into the retrievals. It would therefore be very interesting to see these standard deviations computed as the square root of the sum of the variances divided by the number of samples. How much additional lidar ratio uncertainty is introduced by the use of depolarization ratios to derive total backscatter coefficients.

AR: Thanks for the suggestion.

We calculated the "standard error of the mean (SEM)" of the variables in Table 1, as the square root of the sum of the variances divided by the number of samples, to replace the previous standard deviations in Table 1 (Table 2 in the revised manuscript). Thanks for this inspiration that it would be more meaningful to present the SEMs here, which can represent uncertainties, as the value distributions (also hinted by standard deviations) has been shown by the boxplots in Figure 7 (Figure 8 in the revised manuscript).

In the aspects of how much the additional lidar ratio uncertainties introduced by depolarization ratio correction, under this methodology (assuming a constant of 0.15 at 355 nm), we add this part to a new dedicated section "**4.3 Caveats and uncertainties**":

"With respect to step (4), the assumption of a constant linear depolarization ratio for backscatter coefficient and lidar ratio correction was based on the observations reported by Hu et al. (2022) and corresponding CALIOP measurements. It should be noted that this constant may vary depending on the characteristics of distinct smoke events. The assumption could introduce additional uncertainties. Regarding the calculation of uncertainties in the total backscatter coefficient and lidar ratio resulting from the depolarization ratio correction, the relevant formulas can be derived using equations (1) and (2), as shown below:

$$\sigma_{\beta_{smo}} = \frac{2\beta_{Aeolus}}{1-\delta_{smo,lin}} \cdot \sigma_{\delta_{smo,lin}} \quad (3)$$

$$\sigma_{L_{smo}} = \frac{2\frac{\alpha_{Aeolus}}{\beta_{Aeolus}}}{(1+\delta_{smo,lin})^2} \cdot \sigma_{\delta_{smo,tin}} \quad (4)$$

Among them, α_{Aeolus} and β_{Aeolus} are the extinction and backscatter coefficients observed by Aeolus, while $\delta_{smo,lin}$ and $\sigma_{\delta_{smo,tin}}$ represent the smoke linear depolarization ratio and its corresponding uncertainty, respectively. Using these two formulas, the uncertainties of the total backscatter coefficient ($\sigma_{\beta_{smo}}$) and the lidar ratio ($\sigma_{L_{smo}}$) can be obtained.

Utilizing these formulas, the uncertainties within a single smoke layer captured by one Aeolus cross-section as well as those across different transport phases, will be discussed as follows. First, to investigate the uncertainties introduced by depolarization ratio, assuming α_{Aeolus} of 200 Mm^{-1} and β_{Aeolus} of 3 $Mm^{-1}sr^{-1}$ as constants, under both circumstances. $\delta_{smo,lin}$ is set to the assuming constant of 0.15. For the uncertainty within a single cross-section, $\sigma_{\delta_{smo,tin}}$ of 0.085 is adopted, derived from the standard deviations of sub-regions presented in Table 1. Applying formulas (3) and (4), $\sigma_{\beta_{smo}}$ and $\sigma_{L_{smo}}$ are computed as 0.6 $Mm^{-1}sr^{-1}$ and 8.6 sr, respectively. Although this estimation is contingent upon specific assumptions and the use of CALIOP-derived $\sigma_{\delta_{smo,tin}}$, this approximate uncertainty quantification demonstrates that $\sigma_{\beta_{smo}}$ and $\sigma_{L_{smo}}$ per data bins attributable to $\sigma_{\delta_{smo,tin}}$ may exceed the uncertainties within a single cross-section (as indicated by the standard errors of the mean listed in Table 1). It should be illustrated that the standard errors of the mean in Table 2 do not incorporate the uncertainty estimation described above, as no accurate depolarization information was available for the Aeolus observations. As for the uncertainties introduced by depolarization ratio across different transport phases, the $\sigma_{\delta_{smo,tin}}$ is set to 0.009, which is the largest deviation from the mean depolarization ratio values presented in Table 1. This procedure tests whether the longitudinal changes in the backscatter coefficient and lidar ratio discussed in Section 5 remain robust when the variation in the linear depolarization ratio is considered. Under this assumption, $\sigma_{\beta_{smo}}$ and $\sigma_{L_{smo}}$ can be calculated as 0.06 $Mm^{-1}sr^{-1}$ and 0.9 sr, respectively, using formulas (3) and (4). Considering the mean lidar ratio values of the different cross-sections shown in Table 2, the maximum variation is around 20 sr. Therefore, under the assumption that $\delta_{smo,lin}$ is 0.15, $\sigma_{\beta_{smo}}$ and $\sigma_{L_{smo}}$ are negligible and will not affect the trends of the mean values across different longitudinal transport phases. In conclusion, while correcting the smoke backscatter coefficient and lidar ratio using $\delta_{smo,lin}$ of 0.15 may introduce additional uncertainties for each data bin (0.6 $Mm^{-1}sr^{-1}$ for backscatter coefficient and 8.6 sr for lidar ratio), the corrected results are used for only the mean value analyses of a single measurement cross-section or a specific sub-region in the following discussion."

2. Validating the results obtained in this investigation is a non-trivial task, as most of the information sources that would typically be used for validation (e.g., coincident retrievals by other space-based sensors) are instead used in constructing the retrievals. And given the temporal offsets between (e.g.) MODIS, VIIRS, and ALADIN, the number of exact coincidences is vanishingly small. But it may be possible for the authors to compare the smoke lidar ratios they report over Europe with co-temporal measurements of 355 nm lidar ratios acquired by EARLINET. (I do not know if 355 nm lidar ratios are routinely retrieved by ground-based systems in North America.) I think this would be an especially interesting exercise, since the authors report smoke lidar ratios in this region that are on the low side of the mean lidar ratios given in Floutsi et al., 2023.

AR: Thanks for the comment.

A dedicated study by Baars et al. (2021) conducted co-temporal profile comparisons between ALADIN and the ground-based lidar PollyXT (a member of EARLINET, can retrieve backscatter coefficient,

extinction coefficient and lidar ratio at 355 nm) on 11 September 2020 above Leipzig, Germany. This study targeted a smoke transport event from the US that closely matches and slightly precedes the transport event examined in the present manuscript. The profile comparisons (shown below) demonstrate good agreement in backscatter coefficient, extinction coefficient, and lidar ratio within the smoke layer. Although based on a single site, this research confirms ALADIN's capability for smoke observation.

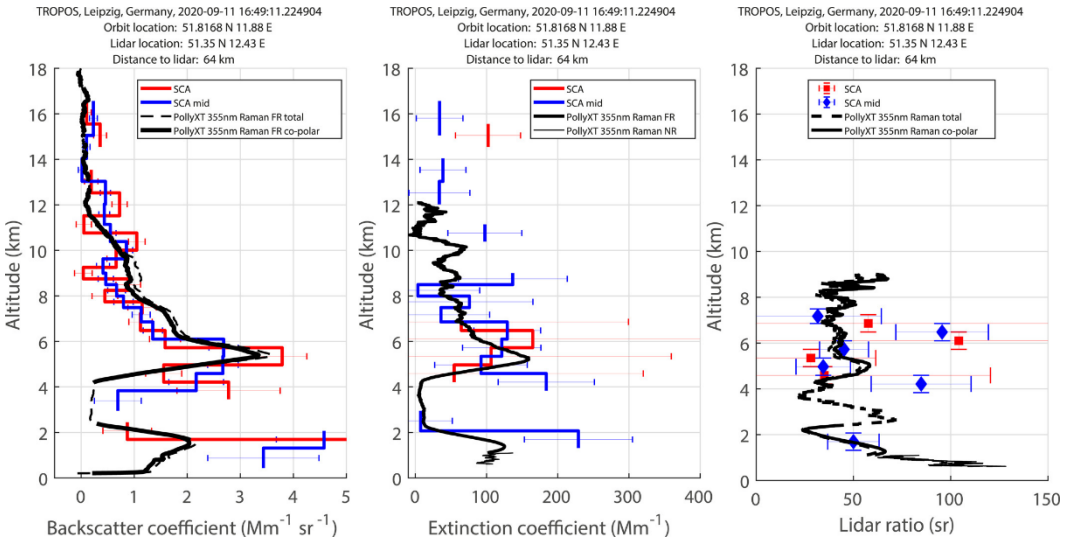

Figure 5 in Baars et al. (2021). Comparison of the optical profiles provided by Aeolus (red and blue) and the ground-based EARLINET lidar PollyXT (black lines). The particle backscatter coefficient (left), the particle extinction coefficient (center), and the corresponding lidar (extinction-to-backscatter) ratio is shown. The ground-based backscatter observations (dashed line) are converted to Aeolus-like, that means, co-polar, profiles (solid line) for comparability. The mean coordinates and distance of the 87 km long Aeolus observations to the ground-based lidar are given as well.

Ground-based lidar (including EARLINET) validation has been demonstrated to be highly significant for the assessment of ALADIN aerosol observation, as shown in Abril-Gago et al. (2022), Gkikas et al. (2023), and Trapon et al. (2025). These studies confirmed the ALADIN's capability for profiling dust, continental and marine aerosol profiling at specific stations as well. For a large-scale aerosol transport event, the limitation of ground-based observations for validation is spatial coverage, as no measurements are available over the ocean, for example. For a transatlantic dust transport event in June 2020, ALADIN aerosol observations were compared with CALIOP, despite a temporal gap of several hours and a limited number of well-matched orbits (Song et al., 2024). To some extent, it demonstrated ALADIN's capability for observing the entire dust transport process. With respect to the smoke transport investigated in this manuscript, we considered using a spaceborne measurement as reference to assess the ALADIN's performance on the entire transport. Considering the scarcity of well-matched orbits, the lack of a cross-polar component in ALADIN backscatter coefficient measurements, and the reliance of CALIOP extinction coefficient retrieval on assumed lidar ratios, we decided to use MODIS for AOD validation. Despite the temporal gap of several hours between ALADIN and MODIS, the averaging of Terra and Aqua MODIS data, together with the statistical results based on a large number of data points (N = 1247, as shown in Figure 4), can provide evidence for ALADIN validation to some extent. The reason for selecting MODIS observations as the reference for this smoke transport event has been summarized from the above discussion and added to the beginning of Section 4.4, "Validation of the Aeolus Smoke

Dataset.": "The performance of ALADIN aerosol profiles has been examined and demonstrated in several validation studies, including Baars et al. (2021), Abril-Gago et al. (2022), Gkikas et al. (2023), and Trapon et al. (2025). Among these, Baars et al. (2021) conducted co-temporal profile comparisons between ALADIN and a ground-based lidar and confirmed ALADIN's capability for profiling backscatter coefficient, extinction coefficient, and lidar ratio within a smoke layer. This smoke layer was transported from the US, and its transport closely matches and slightly precedes the transport event examined in the present study. Nevertheless, for the purpose of verifying the reliability of the derived Aeolus smoke dataset across the entire transport, spaceborne measurement provide data with much larger spatial coverage compared to ground-based lidars, which are limited to specific stations. For a transatlantic dust transport event in June 2020, ALADIN aerosol observations were compared with CALIOP, despite a temporal gap of several hours and a limited number of well-matched orbits (Song et al., 2024). Considering the scarcity of well-matched orbits, the lack of a cross-polar component in ALADIN backscatter coefficient measurements, and the reliance of CALIOP extinction coefficient retrieval on assumed lidar ratios, we decided to use MODIS for AOD validation. Despite the temporal gap of several hours between ALADIN and MODIS, the averaging of Terra and Aqua MODIS data, together with the statistical results based on a large number of data points (N = 1247, as shown in Figure 4), can provide evidence for ALADIN validation to some extent."

It also should be noted that MODIS data were not involved in constructing the retrievals, but only for the validation. To clarify the methodology and procedures introduced in Section 4, a new flowchart has been added as Figure 3:

"The brief flowchart of the methodology introduced in this section is summarized in Figure 3.

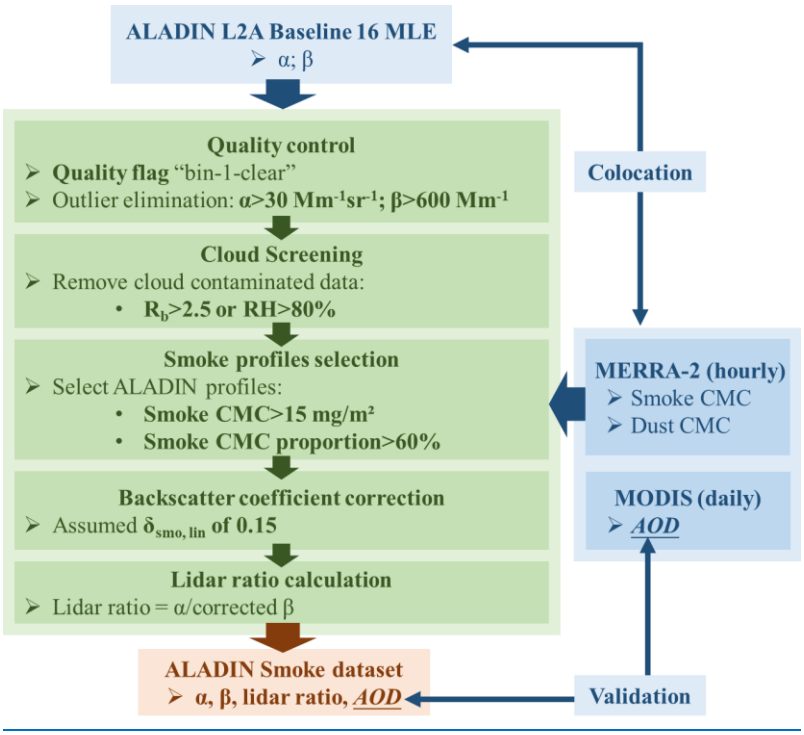

Figure 3. Methodology flowchart for development and validation of the Aeolus-based smoke dataset. α and β represent ALADIN observed extinction and backscatter coefficients. Rb and RH represent backscattering ratio and relative humidity. CMC is column mass concentration and $\delta_{smo,\,lin}$ is smoke linear depolarization ratio."

The fact that the lidar ratios of this smoke transport event are on the low side of the mean lidar ratios reported in Floutsi et al. (2023) could result from the smoke aerosol characteristics themselves, as smoke lidar ratios can vary from 30 sr to 110 sr at 355 nm in the troposphere (Ansmann et al., 2021). Supporting this, Figure 5 in Baars et al. (2021) (shown above) also shows smoke lidar ratios of approximately 40 sr, observed for a smoke layer in a transport event similar to the one in this study. Further discussion on this topic has been added into the relevant part in the new Section 5.1.2 "**Characteristics of the smoke layers at different transport stages**", associated with No.4 of your major comments:

"As for the variations in the lidar ratio, one of the intensive properties that is independent of aerosol concentrations, it presents the properties of smoke particles at different transport stages. The mean lidar ratios ranged from 44 sr to 62 sr, consistent with the broad range of tropospheric smoke lidar ratios (30-110 sr), summarized in Ansmann et al. (2021). A general declining trend from 62 sr on 14 September to 44 sr on 19 September was observed as the smoke transported from the west US to the mid-Atlantic. This decline is considered attributed to the aging process of smoke aerosols, aligning with the findings and the statements in Nicolae et al. (2013), Haarig et al. (2018), Nicolae et al. (2026) and Haarig et al. (2026). Taking 44±2.9 sr on 19 September 2020 as the lidar ratio for aged smoke, this value agrees well with the 40-50 sr reported in Baars et al. (2021) and the 40 ± 6 sr reported in Hu et al. (2022) for aged smoke layers from the similar transport event mentioned above. Subsequently, after being transported to Europe and appearing above cloud layers, the mean lidar ratios turned to increase to around 60 sr on 20 and 21 September, a change that may be explained by hygroscopic growth. During the initial stages of the transport event (14-18 September), the smoke layers gradually became drier, with mean relative humidity from 43 % to 39 %. However, on 20 and 21 September, after the smoke had been transported over Europe and appeared above clouds, the relative humidity of the smoke layers increased to approximately 60%. The lidar ratio and relative humidity exhibited consistent increasing trends on 20 and 21 September. Regarding the extinction coefficient, it increased from 155 Mm-1 to around 200 Mm-1, while the backscatter coefficient remained relatively stable. This suggests that the increase in relative humidity enhanced the smoke lidar ratio, given that the lidar ratio is calculated as the extinction coefficient divided by the backscatter coefficient. A similar phenomenon has been observed and discussed for continental aerosols in Haarig et al. (2025)."

References:

Abril-Gago, J., Guerrero-Rascado, J. L., Costa, M. J., Bravo-Aranda, J. A., Sicard, M., Bermejo-Pantaleón, D., Bortoli, D., Granados-Muñoz, M. J., Rodríguez-Gómez, A., Muñoz-Porcar, C., Comerón, A., Ortiz-Amezcua, P., Salgueiro, V., Jiménez-Martín, M. M., and Alados-Arboledas, L.: Statistical validation of Aeolus L2A particle backscatter coefficient retrievals over ACTRIS/EARLINET stations on the Iberian Peninsula, Atmos. Chem. Phys., 22, 1425–1451, https://doi.org/10.5194/acp-22-1425-2022, 2022.

Ansmann, A., Ohneiser, K., Mamouri, R.-E., Knopf, D. A., Veselovskii, I., Baars, H., Engelmann, R., Foth, A., Jimenez, C., Seifert, P., and Barja, B.: Tropospheric and stratospheric wildfire smoke profiling with lidar: mass, surface area, CCN, and INP retrieval, Atmos. Chem. Phys., 21, 9779–9807, https://doi.org/10.5194/acp-21-9779-2021, 2021.

Baars, H., Radenz, M., Floutsi, A. A., Engelmann, R., Althausen, D., Heese, B., et al. (2021). Californian wildfire smoke over Europe: A first example of the aerosol observing capabilities of Aeolus compared to ground-based lidar. Geophysical Research Letters, 48, e2020GL092194. https://doi.

org/10.1029/2020GL092194.

Floutsi, A. A., Baars, H., Engelmann, R., Althausen, D., Ansmann, A., Bohlmann, S., Heese, B., Hofer, J., Kanitz, T., Haarig, M., Ohneiser, K., Radenz, M., Seifert, P., Skupin, A., Yin, Z., Abdullaev, S. F., Komppula, M., Filioglou, M., Giannakaki, E., Stachlewska, I. S., Janicka, L., Bortoli, D., Marinou, E., Amiridis, V., Gialitaki, A., Mamouri, R.-E., Barja, B., and Wandinger, U.: DeLiAn – a growing collection of depolarization ratio, lidar ratio and Ångström exponent for different aerosol types and mixtures from ground-based lidar observations, Atmos. Meas. Tech., 16, 2353–2379, https://doi.org/10.5194/amt-16-2353-2023, 2023.

Gkikas, A., Gialitaki, A., Binietoglou, I., Marinou, E., Tsichla, M., Siomos, N., Paschou, P., Kampouri, A., Voudouri, K. A., Proestakis, E., Mylonaki, M., Papanikolaou, C.-A., Michailidis, K., Baars, H., Straume, A. G., Balis, D., Papayannis, A., Parrinello, T., and Amiridis, V.: First assessment of Aeolus Standard Correct Algorithm particle backscatter coefficient retrievals in the eastern Mediterranean, Atmos. Meas. Tech., 16, 1017–1042, https://doi.org/10.5194/amt-16-1017-2023, 2023.

Haarig, M., Ansmann, A., Baars, H., Jimenez, C., Veselovskii, I., Engelmann, R., and Althausen, D.: Depolarization and lidar ratios at 355, 532, and 1064 nm and microphysical properties of aged tropospheric and stratospheric Canadian wildfire smoke, Atmos. Chem. Phys., 18, 11847–11861, https://doi.org/10.5194/acp-18-11847-2018, 2018.

Haarig, M., Engelmann, R., Baars, H., Gast, B., Althausen, D., and Ansmann, A.: Discussion of the spectral slope of the lidar ratio between 355 and 1064 nm from multiwavelength Raman lidar observations, Atmos. Chem. Phys., 25, 7741–7763, https://doi.org/10.5194/acp-25-7741-2025, 2025.

Haarig, M., Baars, H., König, L., Donovan, D. P., Ansmann, A., Khaykin, S., et al. (2026). The life cycle of a stratospheric smoke plume as seen from EarthCARE—tracking a plume from Canada to Europe. Geophysical Research Letters, 53, e2025GL119977. https://doi.org/10.1029/2025GL119977.

Hu, Q., Goloub, P., Veselovskii, I., and Podvin, T.: The characterization of long-range transported North American biomass burning plumes: what can a multi-wavelength Mie–Raman-polarization-fluorescence lidar provide?, Atmos. Chem. Phys., 22, 5399–5414, https://doi.org/10.5194/acp-22-5399-2022, 2022.

Nicolae, D., A.Nemuc, D.Müller, C.Talianu, J.Vasilescu, L.Belegante, and A.Kolgotin (2013), Characterization of fresh and aged biomass burning events using multiwavelength Raman lidar and mass spectrometry, J. Geophys. Res. Atmos., 118, 2956–2965, doi:10.1002/jgrd.50324.

Nicolae, D., Ciocan, G.-A., Nemuc, A., Nicolae, V., Talianu, C., Vasilescu, J., Dandocsi, A., Radu, C., Cazacu, M.-M., Vulturescu, V., and Belegante, L.: Examining the characteristics of aerosols: a statistical analysis based on a decade of lidar and photometer observations at the Eastern border of ACTRIS, Atmos. Meas. Tech., 19, 1179–1199, https://doi.org/10.5194/amt-19-1179-2026, 2026.

Song, R., Povey, A., and Grainger, R. G.: Characterization of dust aerosols from ALADIN and CALIOP measurements, Atmos. Meas. Tech., 17, 2521–2538, https://doi.org/10.5194/amt-17-2521-2024, 2024.

Trapon, D., Baars, H., Floutsi, A. A., Bley, S., Haarig, M., Lacour, A., Flament, T., Dabas, A., Nehrir, A. R., Ehlers, F., and Huber, D.: Cross-validations of the Aeolus aerosol products and new developments with airborne high-spectral-resolution lidar measurements above the tropical Atlantic during JATAC, Atmos. Meas. Tech., 18, 3873–3896, https://doi.org/10.5194/amt-18-3873-2025, 2025.

On a related note, I am assuming that the standard deviations reported in Table 1 are the standard

deviations that would be calculated by averaging mean values irrespective of their associated uncertainties. One of the wonderful things about HSRLs is that they can retrieve height-resolved estimates of lidar ratios, whereas elastic backscatter systems like CALIOP can, at best, retrieve layer mean values. However, ALADIN's height-resolved lidar ratio estimates have associated height-resolved uncertainties, and these uncertainties will almost certainly grow larger with the introduction of depolarization ratios into the retrievals. It would therefore be interesting to see these standard deviations computed as the square root of the sum of the variances divided by the number of samples. How much additional lidar ratio uncertainty is introduced by the use of depolarization ratios to derive total backscatter coefficients? How much does this additional uncertainty affect comparisons to EARLINET cotemporal values and/or to the numbers reported in Floutsi et al., 2023? This goes very much to the confidence users should place in the results derived from this data fusion approach.

AR: The quantification of the additional uncertainties introduced by correcting backscatter and lidar ratio with the assumed constant linear depolarization ratio has been conducted in the reply on the last comment. The additional uncertainty on lidar ratio for each data bin was computed as 8.6 sr, while that across different transport phases was 0.9 sr. The uncertainty for each data bin is comparable, compared with the mean observational errors (7.4 sr) provided in Table 1 in Floutsi et al. (2023) (shown below). The uncertainty across the entire transport introduced by the variation of the mean depolarization ratios is low and negligible for the tendencies of the mean lidar ratios in different longitudinal transport phases.

Aerosol type	S_{355}	S_{532}	δ_{355}	δ_{532}	Reference
Ash	51 ± 7.5	48 ± 7.5	36 ± 2.3	–	Groß et al. (2012)*, Sicard et al. (2012), Kanitz (2012)•
Saharan dust	53.5 ± 7.7	53.1 ± 7.9	24.4 ± 2.5	28 ± 1.3	Groß et al. (2011)*,2, Preißler et al. (2011), Kanitz et al. (2013a)•, Baars et al. (2016), Rittmeister et al. (2017)•, Kaduk (2017)6, Haarig et al. (2017a)4, Urbanneck (2018)7, Bohlmann et al. (2018)•, Szczepanik et al. (2021), Haarig et al. (2022)4
Central Asian dust	43.4 ± 1.9	37.7 ± 2.1	22.8 ± 0.8	32.5 ± 0.7	Hofer et al. (2020)5
Middle Eastern dust	39.5 ± 6	37.4 ± 5.3	24.2 ± 2.3	28.4 ± 1.6	Müller et al. (2007)1, Kaduk (2017)6, Urbanneck (2018)7, Filioglou et al. (2020)
Smoke	68.2 ± 7.4	71.8 ± 11.1	2.7 ± 1.3	2.9 ± 0.6	Müller et al. (2007), Baars (2011)3, Tesche (2011)2, Pereira et al. (2014), Giannakaki et al. (2016)3, Janicka et al. (2016), Haarig et al. (2018), Floutsi et al. (2021)8, Ohneiser et al. (2021)9,•
Stratospheric smoke	67.5 ± 19.3	93.8 ± 18.1	22.6 ± 4	17.9 ± 1.7	Haarig et al. (2018), Ohneiser et al. (2020)8
Dust and smoke	72.1 ± 7.7	56.3 ± 6.5	15.7 ± 2	18.9 ± 1.4	Groß et al. (2011)*,2, Tesche (2011)2, Kanitz et al. (2013a)*,•, Giannakaki et al. (2016)3, Kanitz et al. (2014b)•, Kaduk (2017)6, Rittmeister et al. (2017)•
Pollution	51.1 ± 8.7	47.4 ± 7.4	1.1 ± 0.3	2.8 ± 1	Ansmann et al. (2005), Müller et al. (2007), Tesche et al. (2007), Komppula et al. (2012)3, Preißler et al. (2013), Hänel et al. (2012)3, Giannakaki et al. (2016)3, Heese et al. (2017), Kaduk (2017)6, this study (Leipzig)
Dust and pollution	48.5 ± 9.2	46.4 ± 8	15.7 ± 1.7	17.7 ± 2.5	Leipzig, Germany*, Preißler et al. (2013), Janicka et al. (2016), Kaduk (2017)6, Rittmeister et al. (2017)
Dried marine	28 ± 6.6	26.9 ± 10.6	7.5 ± 1.7	8.3 ± 1.1	Haarig et al. (2017b)4, Bohlmann et al. (2018)•
Clean marine	22.4 ± 5.6	21.9 ± 13.4	1.3 ± 0.3	1.4 ± 0.3	Groß et al. (2011)*,2, Kaduk (2017)6, Bohlmann et al. (2018)•, Rittmeister et al. (2017)•
Dust and marine	39.4 ± 5.6	32 ± 7.8	14 ± 1.5	14.7 ± 1.1	Groß et al. (2011)*, Kaduk (2017)6, Bohlmann et al. (2018)• Rittmeister et al. (2017)•
Central European background	57 ± 4.7	56.2 ± 8.3	3.4 ± 1.8	3.2 ± 0.1	Leipzig, Germany, Müller et al. (2007), this study (Leipzig)

Table 1 in Floutsi et al. (2023). Overview of the lidar-derived optical properties of different aerosol types. The lidar ratio S is expressed in steradians (sr) and the particle linear depolarization δ in percent (mean values) along with the mean observational errors. References for each category are given in the right column. Measurements conducted in a field campaign are indicated with a number at the reference and explained in the footnote of the table and during a Polarstern or

Meteor cruise with a bullet symbol (•), while the rest are from PollyNET/EARLINET stations. Measurements conducted with a non-TROPOS lidar are accompanied with a star symbol (⋆).
Reference:

Floutsi, A. A., Baars, H., Engelmann, R., Althausen, D., Ansmann, A., Bohlmann, S., Heese, B., Hofer, J., Kanitz, T., Haarig, M., Ohneiser, K., Radenz, M., Seifert, P., Skupin, A., Yin, Z., Abdullaev, S. F., Komppula, M., Filioglou, M., Giannakaki, E., Stachlewska, I. S., Janicka, L., Bortoli, D., Marinou, E., Amiridis, V., Gialitaki, A., Mamouri, R.-E., Barja, B., and Wandinger, U.: DeLiAn – a growing collection of depolarization ratio, lidar ratio and Ångström exponent for different aerosol types and mixtures from ground-based lidar observations, Atmos. Meas. Tech., 16, 2353–2379, https://doi.org/10.5194/amt-16-2353-2023, 2023.

3. Please say something about the use of daytime vs. nighttime data. From figure 8 it is obvious that both are used. But the quality of the nighttime data is much higher than the daytime data. How are these data quality differences reflected in the statistical comparisons? Does each latitudinal section contain approximately the same ratio of daytime vs. nighttime?

AR: According to the "ADM-Aeolus scient report" (acquired from https://www.esa.int/Applications/Observing_the_Earth/FutureEO/Aeolus/Documents_publications, last access: 22 May 2026), the Aeolus orbit was designed as dawn-dusk orbit with a Mean Time of Ascending/Descending Node at 18:00/6:00 (Local Time). The orbit geometry is depicted below. In September 2020, the terminator was approximately vertical, connecting the North and South Poles. Under this configuration, all data used in this manuscript from the Northern Hemisphere were located in illuminated regions. Accordingly, no differences are expected between data from ascending and descending orbits. Furthermore, the lidar's line of sight pointed toward the anti-Sun direction to minimize the contribution of background radiation.

To clarify this issue, the description has been added in Section 2.1 "ALADIN", as "ALADIN operated on a dawn-dusk orbit with an inclination of 97.01°, and mean times of ascending/descending node at 18:00/6:00 (Local Time) (ESA, 2008)." The statement was also added in the first paragraph of Section 5.2 "Features of the entire smoke event", as "It should be noted firstly, according to the orbit configuration, all data used in this section were located close to the terminator but in illuminated regions (ESA, 2008). Accordingly, no differences are expected between data from ascending and descending orbits."

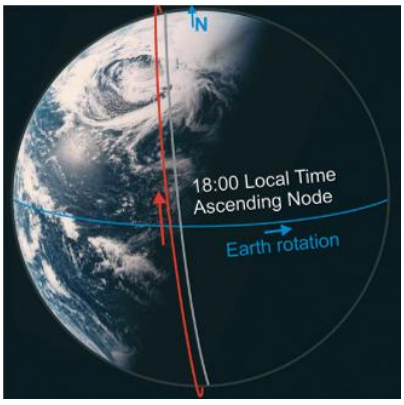

Fig. 4.2 in the "ADM-Aeolus scient report". The Aeolus dusk-dawn orbit of about 400 km altitude (red), and the measurement ground track (grey).

4. I believe the conclusions the authors draw about smoke transport patterns and time-varying smoke optical properties would be buoyed by direct comparisons to other similar transatlantic smoke events; e.g., see the works by Haarig et al., 2018; Hu et al., 2022; Ohneiser et al., 2023; Peterson et al., 2018; and/or Vaughan et al., 2018, which are already cited in the manuscript.

AR: Thanks for the advice. We have addressed the discussion on the comparisons with other similar transatlantic smoke events in these literatures, in Section 5, shown as below.

About **extinction and backscatter coefficient**: "On 20 and 21 September, the mean extinction coefficients are 199 Mm^{-1} and 208 Mm^{-1}, and the mean backscatter coefficients are 3.59 $Mm^{-1}\cdot sr^{-1}$ and 3.87 $Mm^{-1}\cdot sr^{-1}$, which are considered quite high over Europe. In a study targeting a very similar smoke transport event, Hu et al. (2022) reported that a smoke layer transported from the western US was observed by a ground-based lidar over Lille, France, between 22:00 UTC on September 11 and 03:00 UTC on September 12, 2020, with extinction and backscatter coefficients at 355 nm of approximately 180 Mm^{-1} and 5 $Mm^{-1}\cdot sr^{-1}$, respectively. Similarly, Baars et al. (2021) used a ground-based lidar to detect a smoke layer transported from the western US over Leipzig, Germany, on September 11, 2020, reporting extinction and backscatter coefficients at 355 nm of around 160 Mm^{-1} and 3.3 $Mm^{-1}\cdot sr^{-1}$. In both cases, the smoke layers were found in the troposphere (5-7 km), which is comparable to the layer heights observed on September 20 and 21 in this study (7.19 km and 6.89 km, respectively). Although these two cases do not describe transport events identical to the one in the present study, they exhibit extinction and backscatter coefficients similar to those observed here, thereby providing some validation for the ALADIN measurements over Europe. Taken together, these findings suggest that dense smoke plumes originating from the western United States covered Europe on September 11, 12, 20, and 21, 2020."

About **lidar ratio**: "As for the variations in the lidar ratio, one of the intensive properties that is independent of aerosol concentrations, it presents the properties of smoke particles at different transport stages. The mean lidar ratios ranged from 44 sr to 62 sr, consistent with the broad range of tropospheric smoke lidar ratios (30-110 sr), summarized in Ansmann et al. (2021). A general declining trend from 62 sr on 14 September to 44 sr on 19 September was observed as the smoke transported from the west US to the mid-Atlantic. This decline is considered attributed to the aging process of smoke aerosols, aligning with the findings and the statements in Nicolae et al. (2013), Haarig et al. (2018), Nicolae et al. (2026) and Haarig et al. (2026). Taking 44±2.9 sr on 19 September 2020 as the lidar ratio for aged smoke, this value agrees well with the 40-50 sr reported in Baars et al. (2021) and the 40 ± 6 sr reported in Hu et al. (2022) for aged smoke layers from the similar transport event mentioned above. Subsequently, after being transported to Europe and appearing above cloud layers, the mean lidar ratios turned to increase to around 60 sr on 20 and 21 September, a change that may be explained by hygroscopic growth. During the initial stages of the transport event (14-18 September), the smoke layers gradually became drier, with mean relative humidity from 43 % to 39 %. However, on 20 and 21 September, after the smoke had been transported over Europe and appeared above clouds, the relative humidity of the smoke layers increased to approximately 60%. The lidar ratio and relative humidity exhibited consistent increasing trends on 20 and 21 September. Regarding the extinction coefficient, it increased from 155 Mm-1 to around 200 Mm-1, while the backscatter coefficient remained relatively stable. This suggests that the increase in relative humidity enhanced the smoke lidar ratio, given that the lidar ratio is calculated as the extinction coefficient divided by the backscatter coefficient. A similar phenomenon has been observed and discussed for continental aerosols in Haarig et al. (2025)."

About **AOD**: "In general, the total AOD exhibits a decline tendency, dropping from around 0.54 to below

0.33 in the main transport region between 100°W and 20°E. Combining the declining trend in AOD from the Copernicus Atmosphere Monitoring Service model-from 0.5 over the western United States to 0.2 over Europe-during a similar smoke transport event in September 2020 reported by Ceamanos et al. (2023), and comparing both this event and the current study with a tropospheric transatlantic smoke transport event in 2019 from Canada to Europe, where AOD declined from 0.25 to 0.013 as reported by Shang et al. (2024), it can be inferred that the September 2020 smoke transport event was fairly severe."

5. In section 4.3 and figure 4, the authors spend some time and manuscript real estate to comparisons of 355 nm Aeolus optical depths to 550 MODIS optical depths. Given the spectral differences in optical depth between 355 nm and 532 nm, I do not find this especially helpful. I believe readers would be better served if the wavelength conversion was done for all panels in figure 4, not just panel (d). Furthermore, I question the author's choice of the Ångström exponent (Å340-500 = 0.2) used to compare scaled Aeolus AOD at 355 nm to an approximation of the MODIS AOD at 550 nm. Why that value rather than the Å355-532 = 0.5 ± 0.3 reported in Hu et al., 2022?

AR: Thanks for your advice. We conducted wavelength conversion for all panels in Fig. 4 in the revised manuscript. Thanks for the reminding of the choice of the Ångström exponent. In the revised manuscript, we change the use of $Å_{340\text{-}500}$ = 0.2 to $Å_{355\text{-}532}$ = 0.5. The associated description has also been revised. This part is shown as below:

"The dataset covers the period from 11 to 21 September 2020, and the spatial range is from 140°W to 40°E and 20°N to 70°N. Considering that ALADIN (355 nm) and MODIS (550 nm) AOD are in different wavelength and only smoke AOD is compared, the wavelength conversion was conducted. The Ångström exponent of 0.5 was applied to the conversion from 355 nm to 532 nm ($ÅE_{355\text{-}532}$), as reported by Hu et al. (2022) for the same smoke event. The low $ÅE_{355\text{-}532}$ suggests that the smoke plumes could be dominated by the coarse mode aerosols. We also consider it acceptable to use $ÅE_{355\text{-}532}$ for a similar wavelength range (355 nm to 550 nm), assuming the Ångström exponent is constant within the range of 355 nm to 550 nm. The conversion was accomplished using the following formula:

$$AOD_{550\,nm} = AOD_{355nm}\exp(ÅE_{355-532} ln\frac{355}{550}) \quad (2)$$

Basically, the scatter between the MODIS and ALADIN AOD both at 550 nm is presented in Fig. 4 (a), indicating a reasonable degree of agreement, given their distinct measurement techniques, different spatial grids and overpass times. It is evident that the ALADIN AODs are generally less than 1.5 when MODIS AODs range from 1.5 to 3, illustrating that MODIS AODs exceed ALADIN AODS under relatively high AOD conditions. To investigate more specifically, based on these features, we separated the AODs into two groups according to their values. The low AOD group consists of AOD values below 1, while the high AOD group comprises either ALADIN or MODIS AOD values above 1. The AOD deviations between the ALADIN and MODIS measurements for the low and high AOD groups are presented in the histograms in Fig. 4(b) and Fig. 4(c). With respect to the low AOD group, the number of matched pairs (N) is 916 while mean bias (BIAS) is -0.024 and mean absolute error (MAE) is 0.19. These results indicate good agreement and suggest that, compared with MODIS, the Aeolus smoke dataset can provide reliable AOD and extinction coefficient when AOD is below 1. For the high AOD group, N is 331, with a BIAS of -0.459 and a MAE of 0.72. It has been reported that during severe smoke events, MODIS AOD (derived using either the Deep Blue or Dark Target algorithm) may overestimate the AOD under high AOD conditions (Gumber et al., 2023). This finding could explain the

overestimation of MODIS AOD observed in this study.

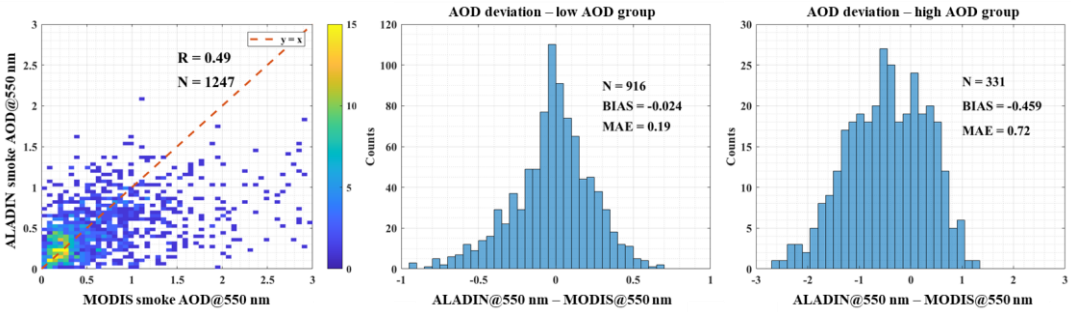

Figure 4. Comparison results between converted ALADIN AOD and MODIS AOD, both at 550 nm. (a) Scatter of MODIS and ALADIN AOD. AOD deviation histograms of ALADIN AOD minus MODIS AOD for (b) high AOD group and (c) low AOD group."

Comments addressed on the manuscript:

1. "In this study, we used the merged "Deep Blue/Dark Target" AOD at 550 nm from both Terra and Aqua to get the best coverage". Please explain how and why this merging was done. What are the potential consequences of averaging AOD retrievals acquired at 12 hour intervals?

AR: The merging was done by averaging the daily AOD at 550 nm from both Terra and Aqua, to get a "merged" Terra and Aqua AOD with larger spatial coverage. This "merged" AOD is considered the daily product derived from MODIS observation. To better clarify, the sentence has been revised as "In this study, we used the merged "Deep Blue/Dark Target" AOD at 550 nm by averaging the daily MODIS AOD from both Terra and Aqua to get the best spatial coverage, for the purpose of smoke plume localization and Aeolus products' validation (Levy et al., 2013)."

2. "The hourly column mass concentration (CMC) of organic carbon, black carbon and dust with the spatial resolution of 0.5°×0.625° from MERRA-2 were utilized to extract smoke data of ALADIN observations." How accurate are these values and how are they validated? Is there any cross-pollination between the passive sensors and the model? i.e., does MERRA2 ingest MODIS or VIIRS data to derive its CMC estimates?

AR: The comprehensive validation of MERRA-2 aerosol column mass concentration was conducted in

Buchard et al. (2017). Good performance for MERRA-2 aerosol column mass concentration was found compared to ground-measurements. MERRA-2 ingest MODIS to derive the CMC estimates. However, MERRA-2 CMC are used for deriving ALADIN observation while MODIS AOD are used for validating ALADIN smoke AOD. They were involved in two relatively isolate procedure and are considered not repeated with each other. We also added this reference below into the revised manuscript.

Buchard, V., and Coauthors, 2017: The MERRA-2 Aerosol Reanalysis, 1980 Onward. Part II: Evaluation and Case Studies. J. Climate, 30, 6851–6872, https://doi.org/10.1175/JCLI-D-16-0613.1.

3. line 182: "a clearly visible, dense smoke plume". I would appreciate reading a word or two (or having a literature citation) explaining how smoke is differentiated from other aerosols in the MODIS and VIIRS measurements.

AR: The statement has been revised as "In panel (a) of Fig. 1, the red dashed region highlights a clearly visible, dense aerosol plume over the west coast, which is likely smoke originating from wildfires in the western US."

4. line 212: “within the altitude of 2 to 15 km”. What motivated the choice of 2 km as the lower boundary? Surely there is plenty of smoke below 2 km.

AR: Altitudes below 2 km are considered too close to the planetary boundary layer, where smoke plume may become mixed with continental or marine aerosol. Therefore, we selected 2 km as the lower boundary to focus on the smoke transport, which primarily occurred in the free troposphere (above 2 km), and to avoid interference from continental and marine aerosol. The analyses in Section 5.2 “Characteristics of the smoke aerosol plume across its entire transport,” also adopt 2 km as the lower boundary for the ALADIN smoke observations.

5. line 225: “AOD data from MODIS”. Repeat question: Is there something in the spectral signature(s) in the MODIS data that specifically identifies aerosols as smoke? Or does the smoke identification come largely from MERRA-2?

AR: We only used MERRA-2 smoke CMC for the smoke identification of ALADIN data. As MERRA-2 assimilates more information, including MODIS, AERONET, etc.

6. line 236 “bin-1-clear”. What information is conveyed by this flag? Readers interested in smoke transport are not necessarily going to be well versed in the Aeolus/ALADIN data products.

AR: The sentence is revised as “The flag “bin-1-clear” (set to 1), indicating normally detected profiles, inside the Aeolus L2A product was used for the preliminary quality control.” to provide sufficient information.

7. line 237: “Backscatter coefficients larger than 30 $Mm^{-1}sr^{-1}$ and extinction coefficients larger than 600 Mm^{-1} were eliminated.” Is the backscatter test applied to the retrieved backscatter for the parallel channel only? The extinction threshold is perhaps unduly restrictive for such a vigorous fire? From Floutsi et al., 2023, AE(355/532) = 1.3 so an extinction threshold of 0.6 per km at 355 nm translates (via equation 3 below) into a threshold of ~0.355 per km at 532 nm. Rather than independent extinction and backscatter thresholds, would it be more effective to invoke a single lidar ratio threshold? If feasible, doing so might permit the inclusion of especially robust smoke samples. In any case, please explain the rationale for specifying these thresholds.

AR: Thanks for the discussion. The backscatter test applied to the retrieved backscatter for the parallel channel only. The AE(355/532)=0.5 was observed in Hu et al. (2022) for this smoke transport and a threshold of ~0.490 per km at 532 nm was set. Considering the smoke lidar ratio can vary over a broad range from 30 sr to 110 sr (Ansmann et al., 2021), it is not easy to adopt a single lidar ratio threshold. The extinction threshold was set more strictly due to the significant challenge of retrieving the extinction coefficient, to avoid outliers as much as possible. The explanation and relevant analyses of outlier elimination has been added in the new Section “4.3 Caveats and uncertainties”, shown as below:

“In step (1), “quality control,” preliminary quality control was conducted using the Aeolus flag and outlier elimination based on thresholds. The principle for threshold setting is that values exceeding than the thresholds are unlikely to originate from typical aerosol cases; they could represent outliers or be contaminated by clouds. After processing the selected Aeolus data (spatial domain: 140°W-40°E, 20°N-70°N; period: 11-21 September 2020) by step (1), 95% of extinction coefficients (174819 out of 183997 data bins) and 95% of backscatter coefficients (175002 out of 183997 data bins) were retained as valid data bins.”

References:

Ansmann, A., Ohneiser, K., Mamouri, R.-E., Knopf, D. A., Veselovskii, I., Baars, H., Engelmann, R., Foth, A., Jimenez, C., Seifert, P., and Barja, B.: Tropospheric and stratospheric wildfire smoke profiling with lidar: mass, surface area, CCN, and INP retrieval, Atmos. Chem. Phys., 21, 9779–9807, https://doi.org/10.5194/acp-21-9779-2021, 2021.

Hu, Q., Goloub, P., Veselovskii, I., and Podvin, T.: The characterization of long-range transported North American biomass burning plumes: what can a multi-wavelength Mie–Raman-polarization-fluorescence lidar provide?, Atmos. Chem. Phys., 22, 5399–5414, https://doi.org/10.5194/acp-22-5399-2022, 2022.

8. line 266: "This variation is presented in Table A1 in the appendix." This is important information that, I think, should be presented as a plot in the main body of the paper. It would also be very helpful to know the number of samples acquired in each region. Do the zonal averages show variations with respect to altitude?

AR: We have moved Table A1 to the main body as Table 1. The data bin counts are also provided in the revised Table 1. While the zonal averages do exhibit variations with altitude, we did not present or discuss this aspect in the manuscript, as our analysis focuses solely on the zonal variation of the lidar ratio, which is related to the depolarization ratio.

9. line 267: "to be in line with the observation of Hu et al. (2022) at 355 nm". I think the authors should offer a more well-developed rationale for their assumption of $d_{lin,355} = 0.15$. According to figure 5b on Hu et al., 2022, the 355 nm linear depolarization ratio reaches 0.15 or above only twice during the nine periods sampled in that work. This observation is reinforced by the text in section 2.3 that says "The PLDRs on 18 and 19 September (P7 and P8) were higher than other days, with the mean PLDR equal to 0.16 at 355 nm, 0.12 at 532 nm and 0.02 at 1064 nm". So for these highly depolarizing layers, $d_{lin,355} \sim 4 \times d_{lin,532} / 3$. Using a mean value of 0.115 (from table A1), this crude approximation yields $d_{lin,355} \sim 0.153$.

AR: Thanks for your detailed analysis. We revised the rationale for the assumption of $\delta_{assu,\,lin}$ at 355 nm according to your suggestion:

"Additionally, the $\delta_{smo,\,lin}$ at 355 nm of 0.16 and the $\delta_{smo,\,lin}$ at 532 nm of 0.12 were observed by Hu et al. (2022) for the same smoke transport event, from which we can derive that $\delta_{smo,\,lin}$ at 355 nm is approximately 1.33 times that at 532 nm. Using a mean value of 0.115 from Table 1, this crude approximation yields that $\delta_{smo,\,lin}$ at 355 nm is approximately 0.15. Therefore, we set the assumed $\delta_{smo,\,lin}$ at 355 nm to 0.15 for the entire transport, considering no anticipated significant zonal variability indicated by the CALIOP observations at 532 nm."

10. line 282: "Therefore, the effect of the assumed constant $\delta_{assu,\,lin}$ on β_{meas} and L_{meas} is considered negligible after averaging within each cross-section or sub-region." I am not convinced by this error analysis. Is the propagation of error a linear function of depolarization ratio uncertainties, or is it nonlinear?

AR: We deleted this rough uncertainty analysis and supplemented a more detailed one in a Section 4.3. Please refer to the Section 4.3 "Caveats and uncertainties" in the revised manuscript.

11. line 287: "15 September 2020". Please also include GMT start and stop times.

Figure 3: "please include longitudes on the x-axis labels and add an orbit track map for spatial context".

AR: Thanks for the suggestion. We have revised the figure and relevant description accordingly:

"One cross-section example that was processed using the five steps above and the corresponding orbit is

shown in Fig. 3. Panel (a) shows aerosol extinction coefficients of Aeolus crossing the smoke plume on 15 September 2020. The cross-section started at 11:51:59 (UTC) on 70.0°N, 75.8°W and ended at 12:04:47 (UTC) on 20.5°N, 91.1°W, crossing the eastern US on a descending orbit. The black bins indicate the invalid values while the gray ones indicate the cloud contaminated bins. They were all removed for subsequent characterization. Within the red dashed lines, the "smoke profiles" captured a thick smoke layer alongside a cloud layer. The maximum altitude was around 10 km, and the latitude range was 33°N to 48°N (with a meridional width of more than 1500 km).

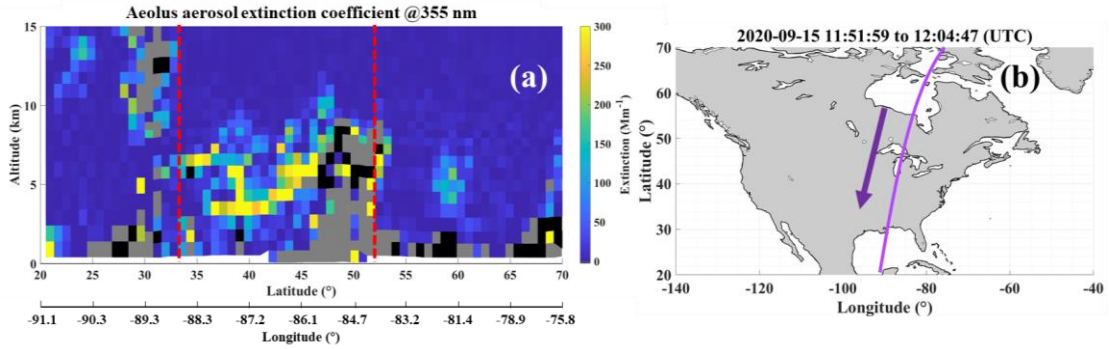

Figure 3. (a) One cross-section example of Aeolus aerosol extinction coefficient crossing the smoke plume, on 15 September 2020, starting at 11:51:59 (UTC) on 70.0°N, 75.8°W and ending at 12:04:47 (UTC) on 20.5°N, 91.1°W. (b) The corresponding descending orbit indicated by the purple curve (Aeolus orbit) and the purple arrow (Aeolus flight direction). The data in panel (a) has been processed to derive smoke data from Aeolus by the steps introduced in the section "Derivation of the smoke dataset from ALADIN observations". The black bins indicate the invalid values, while the grey ones indicate the cloud contaminated bins. The profiles inside two red dashed lines are the "smoke profiles"."

12. line 303: "It is evident that the ALADIN AODs are generally less than 2 when MODIS AODs range from 2 to 3". Does ALADIN typically probe optical depths greater than 2 during daytime? At what point is the ALADIN signal considered to be totally attenuated? A reference to the paper describing the ALADIN layer detection algorithm would be very helpful.

AR: According to "ADM-Aeolus L2A Algorithm Theoretical Baseline Document" (https://earth.esa.int/eogateway/documents/20142/37627/Aeolus-L2A-Algorithm-Theoretical-Baseline-Document.pdf, last access: 28 May 2026), "Some sensitivity tests have shown that the beam gets almost fully attenuated for cloud optical depth strictly larger than 5." indicates that the ALADIN signal was not likely to be totally attenuated when the atmospheric optical depth less than 5. In view of the response to your No.3 major comment, "according to the orbit configuration, all data used in this section were located close to the terminator but in illuminated regions (ESA, 2008). Accordingly, no differences are expected between data from ascending and descending orbits.", we think there was no significant difference between daytime data and nighttime data. Therefore, we consider that "the ALADIN AODs are generally less than 2 when MODIS AODs range from 2 to 3" was not due to the totally attenuation of ALADIN signal.

Reference:

ESA: ADM-Aeolus Science Report, ESA SP-1311, 121 pp., European Space Agency, ISBN 978-92-9221-404-3, https://esamultimedia.esa.int/multimedia/publications/SP-1311/SP-1311.pdf (last access: 22 May

2026), 2008.

13. line 366: “However, the forward trajectory simulations underestimated the height of the smoke layer compared to the Aeolus observations”. Please add a reference to the paper(s) defining the ALADIN layer detection algorithm, its sensitivities, and its uncertainties.

AR: This sentence has been revised as “However, the limited forward trajectory simulations may not adequately represent the ascending motion of the smoke layer compared to what was observed by ALADIN.” The “ADM-Aeolus L2A Algorithm Theoretical Baseline Document” (Flamant et al., 2022) has been supplemented in Section 2.1 “ALADIN” for detailed algorithm introduction.

Reference:

Flamant, P., Dabas, A., Martinet, P., Lever, V., Flament, T., Trapon, D., Olivier, M., Cuesta, J., and Huber, D.: Aeolus L2A Algorithm Theoretical Baseline Document, Particle optical properties product, Tech. rep., ESA, version 6.0, https://earth.esa.int/eogateway/documents/20142/37627/Aeolus-L2A-Algorithm-Theoretical-Baseline-Document.pdf (last access: 28 May 2026), 2022.

14. line 368: “backscatter ratio”. Total backscatter coefficient, yes? Should readers assume the these plots are based solely on data averaging and hence do not account for uncertainties in the assumed depolarization ratio?

AR: Yes, total backscatter coefficient. Revised as “total backscatter coefficient” here. The statement has also been added as “The additional uncertainties of the corrected total backscatter coefficient introduced by the assumed depolarization ratio are discussed in Section 4.3, but are not included in Fig.7 and Table 2.”

15. line 372: “It should be noted that only Aeolus smoke data bins with an extinction greater than 30 Mm^{-1} and a backscatter greater than 1 $Mm^{-1}sr^{-1}$ were considered representative of smoke layers and used in the statistical calculation.” Please explain the rationale for imposing these limits.

AR: The rationale has been added: “These thresholds are set to filter out low noisy values, which can be observed in the clear sky region of the cross-section presented in Fig.3 (a), so that the remaining values above the threshold are considered representative for the smoke layers.”

16. Figure 7: “lidar ratio”. According to Floutsi et al., 2023, these lidar ratios appear unusually low. are there correlative 355 nm measurements by EARLINET that would support these lower values for this event?

AR: More detailed discussion on smoke lidar ratio are supplemented here:

“As for the variations in the lidar ratio, one of the intensive properties that is independent of aerosol concentrations, it presents the properties of smoke particles at different transport stages. The mean lidar ratios ranged from 44 sr to 62 sr, consistent with the broad range of tropospheric smoke lidar ratios (30-110 sr), summarized in Ansmann et al. (2021). A general declining trend from 62 sr on 14 September to 44 sr on 19 September was observed as the smoke transported from the west US to the mid-Atlantic. This decline is considered attributed to the aging process of smoke aerosols, aligning with the findings and the statements in Nicolae et al. (2013), Haarig et al. (2018), Nicolae et al. (2026) and Haarig et al. (2026). Taking 44±2.9 sr on 19 September 2020 as the lidar ratio for aged smoke, this value agrees well with the 40-50 sr reported in Baars et al. (2021) and the 40 ± 6 sr reported in Hu et al. (2022) for aged smoke layers from the similar transport event mentioned above. Subsequently, after being transported to

Europe and appearing above cloud layers, the mean lidar ratios turned to increase to around 60 sr on 20 and 21 September, a change that may be explained by hygroscopic growth. During the initial stages of the transport event (14-18 September), the smoke layers gradually became drier, with mean relative humidity from 43 % to 39 %. However, on 20 and 21 September, after the smoke had been transported over Europe and appeared above clouds, the relative humidity of the smoke layers increased to approximately 60%. The lidar ratio and relative humidity exhibited consistent increasing trends on 20 and 21 September. Regarding the extinction coefficient, it increased from 155 Mm^{-1} to around 200 Mm^{-1}, while the backscatter coefficient remained relatively stable. This suggests that the increase in relative humidity enhanced the smoke lidar ratio, given that the lidar ratio is calculated as the extinction coefficient divided by the backscatter coefficient. A similar phenomenon has been observed and discussed for continental aerosols in Haarig et al. (2025).”

17. Figure 7: “height”. What height is this? e.g., is it the maximum height? the mid-layer height? or something else entirely?

AR: Revised as “data bins’ altitude”.

18. line 382: “the smoke layers on 16 and 18 September were obviously higher”. The AOD on the 16th is not noticeably higher than on the 14th and is actually lower than the AOD on the 21st.

AR: Revised as “the smoke layers on 16 and 18 September were obviously higher than those of cross-sections on 15 and 19 September”.

19. line 385: “The high smoke concentrations could result from the potential accumulation of smoke aerosols when they were transported to above the Atlantic. This phenomenon agrees well with the findings from the analysis of the MODIS AOD and MERRA-2 smoke CMC across the entire transport region, as illustrated in Fig. 2 (a) and (b) and the accompanying descriptions.” More explanation needed. Looking at figure 5 (and also at 2b), the column mass concentrations in the daily measurement regions appear to be highest on the 14th and lowest on the 21st, which would appear to be inconsistent with the extinction coefficients reported in table 1 (unless there was a substantial change in mass-to-extinction ratio during transport???)

AR: The mean extinction coefficient on 14 September is the highest, aligning with the highest column mass concentration on the same day. AOD not being the highest may result from the averaging over some regions with relatively low smoke load. The fairly high extinction coefficient (mean and median values) on 21 September may be because of the hygroscopic growth of the smoke particles, which has the same increasing trend as the extinction coefficient and relative humidity. This inconsistency between the ALADIN extinction coefficient and MODIS AOD/smoke CMC could also highlight the capability of smoke observation above clouds by lidar, which cannot be accomplished or assimilated by MODIS and MERRA-2. We considered the feature of AOD variation needs much data involved, thus the AOD in Table 2 were removed and we discuss them in Section 5.2 “Characteristics of the smoke aerosol plume across its entire transport”.

20. line 400: “which could be the reason for the altered lidar ratio”. Should we infer that the uptake of water by the smoke particles increases the lidar ratio?

AR: The discussion on this topic has been extended as:

“Subsequently, after being transported to Europe and appearing above cloud layers, the mean lidar ratios turned to increase to around 60 sr on 20 and 21 September, a change that may be explained by

hygroscopic growth. During the initial stages of the transport event (14-18 September), the smoke layers gradually became drier, with mean relative humidity from 43 % to 39 %. However, on 20 and 21 September, after the smoke had been transported over Europe and appeared above clouds, the relative humidity of the smoke layers increased to approximately 60%. The lidar ratio and relative humidity exhibited consistent increasing trends on 20 and 21 September. Regarding the extinction coefficient, it increased from 155 Mm^{-1} to around 200 Mm^{-1}, while the backscatter coefficient remained relatively stable. This suggests that the increase in relative humidity enhanced the smoke lidar ratio, given that the lidar ratio is calculated as the extinction coefficient divided by the backscatter coefficient. A similar phenomenon has been observed and discussed for continental aerosols in Haarig et al. (2025)."

Reference:

Haarig, M., Engelmann, R., Baars, H., Gast, B., Althausen, D., and Ansmann, A.: Discussion of the spectral slope of the lidar ratio between 355 and 1064 nm from multiwavelength Raman lidar observations, Atmos. Chem. Phys., 25, 7741–7763, https://doi.org/10.5194/acp-25-7741-2025, 2025.

21. line 424: "We believe that Aeolus lidar observations are capable to identify a smoke layer even if thin clouds are present in a given profile". While this may be true, without information from additional sensors it's not at all apparent that these smoke layers could be reliably differentiated from optically thin cloud.

AR: To clarify, it has been revised as "We believe that Aeolus smoke dataset acquired in this paper are capable of observe a smoke layer even if thin clouds are present in a given profile."

22. line 427: ". The Aeolus smoke dataset does not present the transport of the southern plume near the Sahara Desert". Do the CALIOP observations suggest any further extension of the southward plume that is not captured by ALADIN?

AR: The sentence has been revised as "The reason that Aeolus smoke dataset does not present the transport of the southern plume near the Sahara Desert could be that the plume is mixed with dust aerosols, leading to its exclusion from the dataset, as described in Section 4.2." We consider it would be also difficult for CALIOP to observe this southern plume extension as the its mainly located in the low and medium troposphere so that it was easy to be mixed with dust aerosols from the Sahara Desert. But the extension and the potential mixing of smoke (organic carbon) and dust can be inferred from the CMC maps below:

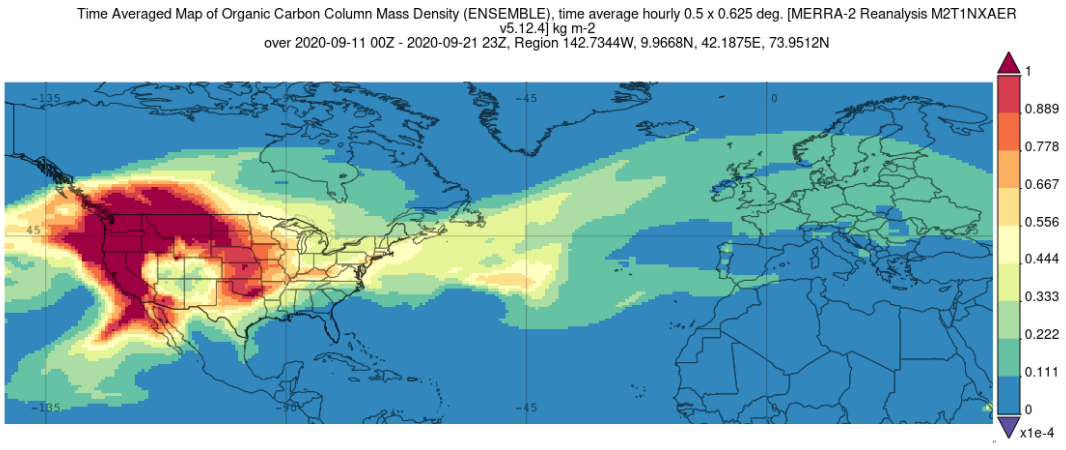

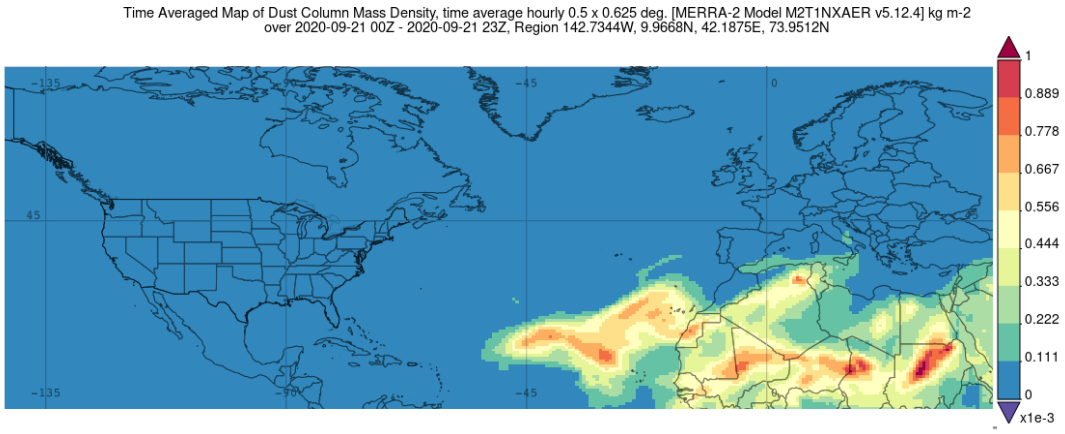

23. Fig 9: Could the sharp increase in AOD between 2 km and 7 km be attributed to misclassification of aerosol types by CALIOP over Europe? With so few data points, I'm reluctant to put much faith in the data at this point.

AR: We added a statement to illustrate this: "Additionally, the sharp increases in AOD and AOD_M may be attributed to the low data count (15), which are considered insufficient to be representative of the observed trend." But it is not considered to be attributed to the misclassification of aerosol types by CALIOP, as we used the MERRA-2 CMC threshold for smoke profiles selection rather than CALIOP.

24. Fig 9:

Since AOD stats are shown as a function of altitude, it would be helpful to show count numbers accumulated within each altitude range. This could be easily done with a stacked bar chart.

How were the altitude statistics compiled? Do the data in figure 9b show means and standard deviations computed over all smoke data bins in each column? Or do they instead show statistics for only the uppermost smoke bin detected in each column? I suspect it's the former, since the data counts shown in figure 9d are substantially larger than those in figure 9c. If this is true, I suspect box and whisker plots would yield a more informative presentation of the results.

AR: Thanks for the advice. We have revised the stacked bar for panel (c), and provided boxplots for smoke bins altitudes in panel (b). Here is the revised figure:

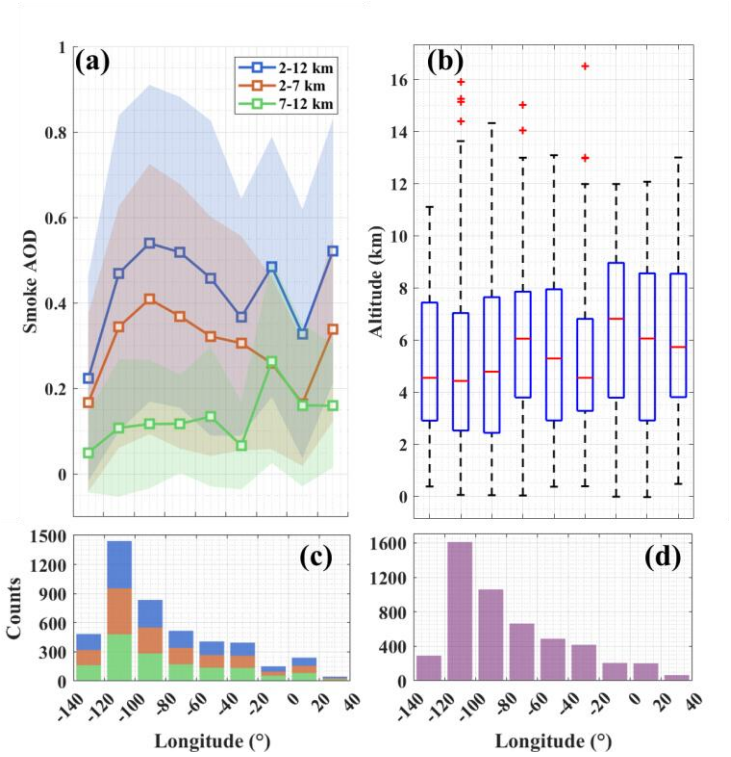

Figure 9. Statistical results (a) smoke AOD (means and standard deviations), (b) smoke bins altitude (boxplot) along longitude. (c)(d) The corresponding data counts of the statistics. The statistics were calculated using the Aeolus smoke dataset in the period of 14 to 21 September 2020, in the smoke plume transport region of 140°W to 40°E and 20°N to 70N, and with the longitude grid of 20°. Smoke AOD includes total AOD (2 km to 12 km), AOD within 2 to 7 km (AOD_M), and AOD within 7 to 12 km (AOD_U), indicated by the blue, red and green curves, respectively. In panel (c), the corresponding data counts are also presented by the stacked bars in the same color with the AOD curves.

25 line 440: "In addition, for all parameters except AOD, only the data bins with extinction greater than 30 Mm^{-1} and backscatter greater than 1 $Mm^{-1}sr^{-1}$ were considered representative of smoke layers and used in the statistical calculation." Why was an exception made for AOD? Please explain the rationale for imposing these limits.

AR: The sentence has been revised as "In addition, only the data bins with extinction greater than 30 Mm^{-1} and backscatter greater than 1 $Mm^{-1}sr^{-1}$ were considered representative of smoke layers and used in the statistical calculation." The rationale was also added as "These thresholds are set to filter out low noisy values, which can be observed in the clear sky region of the cross-section presented in Fig.3 (a), so that the remaining values above the threshold are considered representative for the smoke layers."

26. line 452: "injected". Picky language point: smoke would presumably be "injected" into the UTLS by convection at the source. But aerosols "injected" into the mid-troposphere could later be "lofted" into the upper troposphere during transport.

AR: Revised as "lofted".

27. line 461: "which may be related to the mechanism of the plume separation." Or the scarcity of data samples.

AR: The plume separation is further investigated in detail in the new Section 5.2.2 “Investigation of the two branches following plume separation”.

28. line 485: “starting from the west coast of the US on around 14 September”. FWIW, I suspect the actual start was a week or so earlier. See the CALIOP images at https://www-calipso.larc.nasa.gov/products/lidar/browse_images/show_v451_detail.php?s=production&v=V4-51&browse_date=2020-09-07&orbit_time=10-12-28&page=1&granule_name=CAL_LID_L1-Standard-V4-51.2020-09-07T10-12-28ZN.hdf, which show a pyroCb event injecting smoke into the stratosphere.

AR: Thanks for the investigation. However, we consider that the transport initiated on 7 September 2020 may represent a separate event preceding the one investigated in the current manuscript, and has already been studied by Baars et al. (2021) and Hu et al. (2022).

References:

Baars, H., Radenz, M., Floutsi, A. A., Engelmann, R., Althausen, D., Heese, B., et al. (2021). Californian wildfire smoke over Europe: A first example of the aerosol observing capabilities of Aeolus compared to ground-based lidar. Geophysical Research Letters, 48, e2020GL092194. https://doi.org/10.1029/2020GL092194.

Hu, Q., Goloub, P., Veselovskii, I., and Podvin, T.: The characterization of long-range transported North American biomass burning plumes: what can a multi-wavelength Mie–Raman-polarization-fluorescence lidar provide?, Atmos. Chem. Phys., 22, 5399–5414, https://doi.org/10.5194/acp-22-5399-2022, 2022.

29. line 500: “. We highlight the ability of Aeolus to measurement aerosol layers even if in the presence of thin clouds, providing more information than passive instruments like MODIS, which are sensitive to cloud contamination.” It's still not clear to me how ALADIN alone can distinguish between thin cloud and dense aerosol.

AR: Revised as “We highlight the capability of the Aeolus smoke dataset (derived from ALADIN with the assistance of multi-source data) to observe aerosol layers above clouds, thereby providing more information than passive instruments such as MODIS, which are susceptible to cloud contamination.”